ZOOPLANKTON DISTRIBUTION FROM BACKSCATTER DATA OF ADCP INSTRUMENT IN WEST SUMATRA WATERS

SEBARAN ZOOPLANKTON DARI DATA HAMBURAN BALIK INSTRUMEN ADCP DI PERAIRAN BARAT SUMATERA

Gandhi Napitupulu[1,2*], Rizqi Ayu Farihah[1,2], Henry Munandar Manik[3], Oktavira Dwi Demia Larasati[4], Moses Napitupulu[5], Lamona Irmudyawati Bernawis[1,2], Ivonne Milichristi Radjawane[1,6], Edi Kusmanto[7]

[1]Environmental and Applied Oceanography Research Group, Faculty of Earth Science and Technology, Bandung Institute of Technology, Bandung, Indonesia

[2]Study Program of Oceanography, Faculty of Earth Sciences and Technology, ITB, Cirebon, Indonesia

[3]Department of Marine Science and Technology, Faculty of Fisheries and Ocean Sciences, IPB University, Bogor, Indonesia

[4]Study Program of Earth Science, Faculty of Earth Science and Technology, ITB, Bandung, Indonesia

[5]Study Program of Shipbuilding Engineering, Faculty of Engineering, University of Indonesia, Depok, Indonesia

[6]Korea-Indonesia Marine Technology Cooperation Research Center, ITB, Cirebon, Indonesia

[7]Oceanographic Research Center, National Research and Innovation Agency, Jakarta, Indonesia

*Corresponding author: gandhinapitupulu88@gmail.com

(Received 27 January 2024; in revised from 31 January 2024 accepted 27 November 2024)

DOI : 10.32693/bomg.39.2.2024.871

ABSTRACT: Acoustic Doppler Current Profiler (ADCP) conventionally used to monitor ocean current profiles and potentially detect zooplankton distribution remains largely unexplored. Zooplankton are key consumers in the marine food chain, therefore understanding their distribution is critical. This study aims to map the distribution of zooplankton in West Sumatra waters using ADCP backscatter data. Data analyzed encompass ocean current measurements, backscatter, and conductivity-temperature-depth (CTD) profiles collected from March 1 to 3, 2017. Raw ADCP digital counts were converted into mean volume backscattering strength (MVBS) in dB using sonar equations, proportional to zooplankton biomass. The conversion process involved corrections for sound attenuation due to distance and water absorption, ADCP transducer angle correction, and noise correction. Processing results revealed zooplankton distribution in raw ADCP data ranging from 20 to 160 counts and in MVBS data spanning -140 dB to -40 dB. MVBS values derived from ADCP acoustic signal processing were filtered within the -100 dB to -60 dB range, representing the zooplankton backscatter range. Zooplankton distribution was observed at depths of 0-300 m. Vertical zooplankton distribution was generally high in the 100-200 m layer and decreased at 0-100 m and 200-300 m. This is attributed to the influence of the Equatorial Undercurrent transporting zooplankton biomass from the Indian Ocean to West Sumatra waters at depths of 100-200 m, characterized by high salinity (34.6-35.2 PSU) and cold temperatures (19°-21°C). This study demonstrates the utility of ADCP in observing zooplankton distribution based on their backscatter values and the influence of ocean currents in transporting zooplankton biomass.

Keywords: ADCP, backscatters, detection of zooplankton distribution, West Sumatra

ABSTRAK: *Acoustic Doppler Current Profiler (ADCP) yang secara konvensional digunakan untuk memantau profil arus laut dan berpotensi mendeteksi distribusi zooplankton sebagian besar masih belum dieksplorasi. Zooplankton adalah konsumen utama dalam rantai makanan laut, oleh karena itu memahami distribusinya sangat penting. Penelitian ini bertujuan untuk memetakan*

distribusi zooplankton di perairan Sumatera Barat dengan menggunakan data hamburan balik ADCP. Data yang dianalisis meliputi pengukuran arus laut, hamburan balik, dan profil konduktivitas-suhu-kedalaman (CTD) yang dikumpulkan dari tanggal 1 hingga 3 Maret 2017. Hitungan digital ADCP mentah dikonversi menjadi kekuatan hamburan balik volume rata-rata (MVBS) dalam dB menggunakan persamaan sonar, yang sebanding dengan biomassa zooplankton. Proses konversi melibatkan koreksi untuk pelemahan suara karena jarak dan penyerapan air, koreksi sudut transduser ADCP, dan koreksi kebisingan. Hasil pemrosesan menunjukkan distribusi zooplankton dalam data mentah ADCP berkisar antara 20 hingga 160 cacah dan dalam data MVBS yang berkisar antara -140 dB hingga -40 dB. Nilai MVBS yang berasal dari pemrosesan sinyal akustik ADCP disaring dalam kisaran -100 dB hingga -60 dB, yang mewakili kisaran hamburan balik zooplankton. Distribusi zooplankton diamati pada kedalaman 0-300 m. Distribusi zooplankton secara vertikal umumnya tinggi pada lapisan 100-200 m dan menurun pada lapisan 0-100 m dan 200-300 m. Hal ini disebabkan oleh pengaruh Arus Bawah Khatulistiwa yang mengangkut biomassa zooplankton dari Samudera Hindia ke perairan Sumatera Barat pada kedalaman 100-200 m, yang dicirikan oleh salinitas yang tinggi (34,6-35,2 PSU) dan suhu yang dingin (19 ° -21°C). Penelitian ini menunjukkan kegunaan ADCP dalam mengamati distribusi zooplankton berdasarkan nilai hamburan balik dan pengaruh arus laut dalam mengangkut biomassa zooplankton.

Kata Kunci: *ADCP, hamburan balik, deteksi distribusi zooplankton, Perairan barat Sumatera*

INTRODUCTION

The waters of West Sumatra, Indonesia, harbor a vibrant marine ecosystem teeming with diverse organisms, including zooplankton. These microscopic creatures play a pivotal role in maintaining the delicate balance and productivity of marine ecosystems (Nava & Leoni, 2021). Zooplankton serve as crucial components of the marine food chain, facilitating nutrient cycling and energy transfer (Lomartire et al., 2021). Additionally, their presence serves as an indicator of environmental quality and the stability of aquatic ecosystems (Bakhtiyar et al., 2020).

Monitoring zooplankton distribution in West Sumatra waters is essential for sustainable marine ecosystem conservation and management. Acoustic Doppler Current Profiler (ADCP) technology has gained prominence in monitoring ocean currents and physical water properties (Manik & Firdaus, 2021; Manso-Narvarte et al., 2020). However, harnessing ADCP for zooplankton abundance detection remains an evolving and challenging research frontier (Cheng et al., 2022).

The backscatter signal obtained from ADCP is often attributed to zooplankton biomass, as expressed in MVBS (Mean Volume Backscatter) units (Wormuth et al., 2000). MVBS data can be employed to elucidate various aspects of zooplankton behavior, including average vertical migration rates, migration timing within the observation area (Manik, 2015), migration patterns (Holliday et al., 1989; Receveur et al., 2020), and spatial distribution within the water column relative to currents (Espinasse et al., 2023). Studies have demonstrated that horizontal current velocities significantly influence zooplankton presence in a given water body. Zooplankton exhibit horizontal movement in response to current flow, constrained by their limited mobility (La et al., 2015; Guerra et al., 2019).

Zooplankton identification can be achieved based on MVBS values, as MVBS is a function of population abundance and individual zooplankton target strength (Thoman et al., 2023). Measurements have shown that sound wave propagation time through zooplankton-laden seawater is shorter than in pure seawater. This indicates that sound velocity within zooplankton is slightly faster than in seawater. This phenomenon is attributed to small zooplankton (<1 mm) (Szczucka et al., 2016).

This research aims to utilize ADCP backscatter data for zooplankton detection in West Sumatra waters. By monitoring ocean currents and recording ADCP backscatter data, we seek to unravel the distribution patterns of zooplankton in this region. The Indonesia Prima 2017 program, initiated by the Indonesian Meteorological, Climatological, and Geophysical Agency (BMKG) in 2017, provided a valuable opportunity to collect data from the eastern Indian Ocean (West Sumatra waters) using the Research Vessel Baruna Jaya VIII. Characterizing zooplankton distribution can serve as supporting data for fisheries resource management, potentially

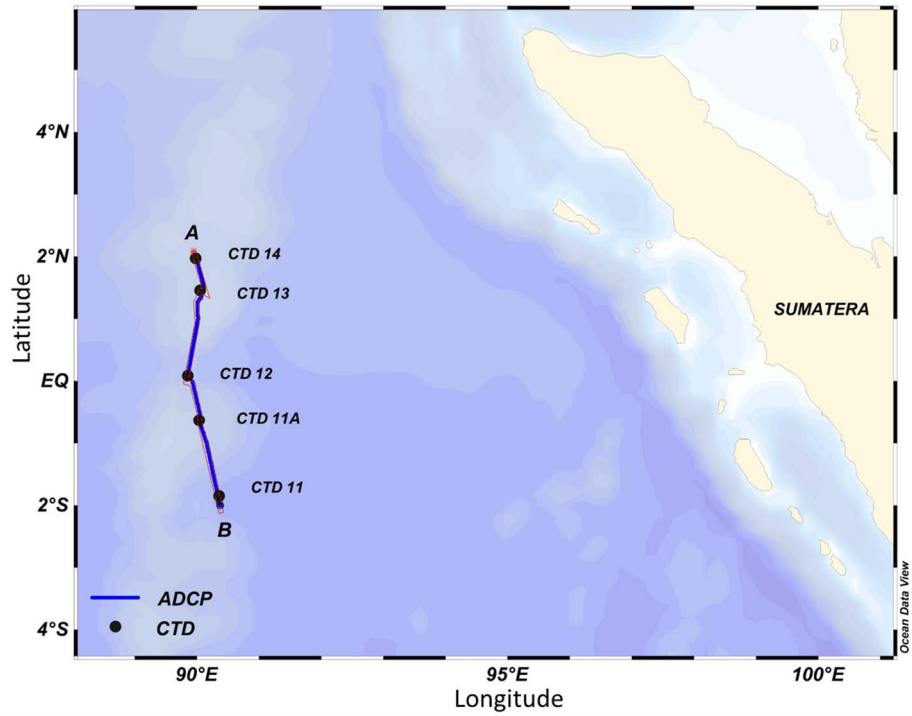

Figure 1. Study area in the western waters of Sumatra

enhancing fish production in West Sumatra waters and the surrounding region.

METHODS

The data used were the results of the Indonesia Prima cruise in the western waters of Sumatra on March 1 to 3, 2017 with latitude 2°00' S to 2°00' N and longitude 90°00' E (Figure 1). Oceanographic data (temperature, salinity, and density) at each observation station were measured continuously using a Conductivity Temperature Depth (CTD) type SBE 911+ Seabird Electronic Inc from the surface (5 m) to 500 m depth. Data were processed using MATLAB to produce temperature, salinity, and density versus time and depth plots and TS diagrams.

Current profiles were recorded continuously using a Shipboard Acoustic Doppler Current Profiler (SADCP) with a frequency of 75 kHz from the surface (5 m) to 500 m depth. This equipment has a blank zone after transmitting of 8 m plus a ship keel of 4.3 m so that the peak measurement depth is 12.3 to 500 m from the surface with a vertical bin every 5 m. Current profile measurements at 2 s intervals were taken along the track from CTD station 11 to CTD 14 with an average vessel speed of 8 knots.

This study used a Teledyne Ocean Surveyor SADCP instrument with a frequency of 76.8 kHz and a bin size of 5 m was used. Echo Intensity with units of counts is the amount of backscatter value read by the ADCP instrument. Estimation of zooplankton abundance can be done by processing the amplitude in units of counts from the ADCP instrument (Chun et al., 2022) to be processed into acoustic backscatter values in the form of mean volume backscattering strength (MVBS) (Cisewski et al., 2010). The configuration used on the SADCP instrument is shown in Table 1.

Table 1. Configuration of the SADCP instrument.

Parameter	SADCP
Frequency (kHz)	76,8
Ping interval (s)	110
Pulse Duration (s)	110
Bin size (m)	5
Transducer tilt angle (°)	20°
Orientation	*Downward-looking*

The acoustic signal returned to the ADCP from the reflection of objects in the water column is called echo intensity (EI) with a value range between 0-255 count (28 or 8 bits of data in digital numbers) in automatic gain control (AGC) (RDI 1990, Cisewski et al., 2016). The RSSI magnitude (received signal strength indicator) is calculated in units of count, which is a dimensionless unit (relative value). RSSI values need to be converted to MVBS to make them absolute and proportional to zooplankton biomass for further analysis (Vogel et al., 2010). The conversion

process considers corrections for sound attenuation due to distance effects, sound absorption by the medium, and eliminating noise's influence (Dwinovantyo et al., 2018). The MVBS calculation is performed by considering the manufacturing system constant (C), the transmitted pulse, and the transmitted power. The MVBS value calculation uses the sonar equation developed by RDI (1990) and Mullison (2017) as shown in Equation (1) and Equation (2):

$$MVBS = C + 10\,log\left((T_x + 273{,}16)R^2\right) - L_{DBM} - P_{DBW} + 2\alpha R + 10\,log\left(10^{\frac{K_c(E-E_r)}{10}} - 1\right) \quad (1)$$

$$MVBS = 10\,log\left((T_x + 273{,}16)R^2\right) - L_{DBM} \mp P_{DW} + 2\alpha R + 10\,log\left(10^{\frac{K_c(E-E_r)}{10}} - 1\right) \quad (2)$$

$MVBS$ (dB/m^3) is the average S_V value in the integration cell. S_V is the ratio between the intensity reflected by a target group (biomass) in the water column (Simmonds & MacLennan, 2008; Mullison, 2019). T_x is the measured temperature internal to the transducer (°C), E is the measured RSSI amplitude of the return signal on the ADCP for each bin along each beam (count), E_r is the relative RSSI amplitude constant determined as the noise level across transducers by calculating the minimum value of EI in the time series data (count), L is the transmitted pulse length (m), K_c is the power output that depends on the system supply voltage at factory calibration (W), L_{DBM} is the logarithmic transmitted wavelength $log(m)$, and P_{DBW} is the logarithmic transmit power $log(W)$.

K_c (dB/count) in Equation (1) and Equation (2) is a constant factor to convert the raw ADCP data from a digital number in the form of a count to dB. K_c is a beam-specific scaling factor with values ranging from 0.35 to 0.55. The K_c value is obtained from the manufacturer's information or $\overline{T_x}$ in Equation (3) obtained during ADCP calibration (Deines, 1999).

$$K_c = \frac{127.3}{T_x + 273{,}16} \quad (3)$$

R (m) in Equation (1) and Equation (2) is the slant range value from the transducer to the center of the bin (where the scattering object is located). ADCP sounding results require correction of the acquisition depth to the transducer slope angle (Deines, 1999; Lee et al., 2008; Schiano et al., 2013).

$$R = \frac{B + \frac{L+D}{2} + (n-1)D + \frac{D}{4}}{\cos\theta} \times \frac{C'}{C_1} \quad (4)$$

where B is the blanking zone distance below the transducer (m), D is the bin size (m), n is the number of bins of the measured scattering layer, C' is the depth-dependent average sound speed from the transducer to the bin (m/s), C_1 is the speed of sound in water used by the ADCP and its value is set during calibration (m/s), and θ is the inclination angle of the beam emitted by the transducer to the vertical axis (°).

The value of the slope range (Equation 4) should not be less than π(R0/4) to be used following the requirement of decreasing wave intensity as it propagates from the source. In addition, the acceptable data range (R_{max}) is as follows (Woodgate & Holroyd, 2011):

$$R_{max} = H \cos\theta \quad (5)$$

where H is the length of distance from the ADCP instrument to the water surface (m).

Before obtaining the value of $\overline{R}$ in Equation (4), we must find the value of C' which is the speed of sound in the water column. This parameter depends on the temperature, salinity, and depth data from CTD measurements that describe the characteristics of the study site waters. The value of C' is obtained from Mackenzie (1981):

$$C' = 1448.96 + 4.591T - 5.304 \times 10^{-2}T^2 + 2.374 \times 10^{-4}T^3 + 1.340(S-35) + 1.630 \times 10^{-2}D + 1.675 \times 10^{-7}D^2 - 1.025 \times 10^{-2}T(S-35) - 7{,}139 \times 10^{-13}TD^3 \quad (6)$$

where T is the temperature value (°C), S is the salinity value (ppt), D is the depth value (m), and α (dB/m) is the attenuation of the acoustic wave signal due to the absorption of energy when the signal propagates in the water column. The value of α is obtained as follows (Ainslie and McColm, 1998):

$$\alpha = 0.106\frac{f_1 f^2}{f^2 + f_1^2}e^{\frac{pH-8}{0.56}} + 0.52\left(1 + \frac{T}{43}\right)\left(\frac{S}{35}\right)\frac{f_2 f^2}{f^2 + f_2^2}e^{-\frac{z}{6}} + 0.00049 f^2 e^{-\left(\frac{T}{27} + \frac{z}{17}\right)} \quad (7)$$

$$f_1 = 0.78\left(\frac{S}{35}\right)^{\frac{1}{2}} e^{\frac{T}{26}} \quad (8)$$

$$f_2 = 42e^{\frac{T}{17}} \quad (9)$$

The value of $\overline{\alpha}$ in Equation (7) can be obtained by first obtaining the values of f_1 in Equation (8) and f_2 in Equation (9). f is the sound frequency of the ADCP instrument (kHz), f_1 is the relaxation frequency of the boron element, f_2 is the relaxation frequency of the magnesium element, z is the depth

value (m), T is the temperature quantity (°C), S is the salinity quantity (ppt), and pH is the degree of acidity.

The value of C (dB) can be obtained from the manufacturer's information provided or can be calculated as follows (Deines, 1999):

$$C = 10\log_{10}\left(\frac{8KFB_N\cos(\theta)}{\pi E_x^2 d^2}\right) \quad (10)$$

where K is Boltzmann's constant (J/°K), B_N is the noise bandwidth (Hz), θ is the tilt angle of the transducer's emitted beam to the vertical axis (°), E_x is the transducer efficiency, F is the receiving system noise factor, and d is the transducer diameter (m).

In the process of converting raw ADCP data into MVBS (dB), there is a transmission loss (TL) variable (dB) that is calculated first before the sonar equation. According to Flagg & Smith (1989), TL is the loss of sound energy with increasing depth as the wave propagates through the medium. It is caused by geometrical spreading and attenuation factors in the form of absorption (Dwinovantyo et al., 2018; Gartner, 2004). This correction aims to equalize the strength of sound energy in all depth layers because energy tends to be strong near the surface and decreases as depth increases. The formulation of the TL variable calculated for depth uses Urick's (1984) equation:

$$TL = 20\log_{10} R + 2\alpha R \quad (11)$$

Table 2. Configuration of ADCP instrument parameters for data processing.

Parameter	Shipboard ADCP
C, system constant (dB)	-164,26
T_x, Transducer temperature (0C)	20
P, wavelength (mm)	20
L_{DBM}, Logarithmic pulse (dB)	13,01
P_{DBW}, logarithmic power (dB)	24
K_c, scale factor (dB count-1)	40
E_r, minimum RSSI value	20
α, absorption coefficient (dB m^{-1})	0,0238
C, speed of sound (ms^{-1})	1475

where α (dB/m) is the absorption coefficient, while R (m) is the slant range. Other parameters required for the formulation of the MVBS conversion in Equation (1) and Equation (2) can be found in Table 2.

The initial process in MVBS computation is that the EI value of each ping is analyzed to remove bad data by eliminating the percent good threshold below 80%. Percent good is a measure of data quality and determines the ratio of good pings per total pings for each ensemble profile. Correction to the slant range was done because the ADCP has a tilt angle of 20° which can bias the actual zooplankton position in MVBS computation (Mohn et al., 2018). MVBS computation produces data in the form of dB values measured at a certain range per unit distance by considering the instrument constant and the system mean square output voltage using the time-varied gain (TVG) function (Kang et al., 2002; Lee et al., 2014).

RESULTS AND DISCUSSIONS

Echo Intensity (EI)

Echo intensity (EI) versus depth in the West Sumatra waters (Figure 2a) ranged from 0 to 200 counts on the automatic gain control (AGC) scale. Zooplankton typically produces acoustic noise between 70 and 160 counts (Lyons & Parish, 1994; Song et al., 2022), indicated by light blue to orange shades, while background noise falls within 20-25 counts (Heywood et al., 1991), shown in dark blue. The central layer with the strongest EI (around 90-100 counts), fluctuating between 40 and 120 m depth, represents the zooplankton biomass deep scattering layer (DSL).

Figures 2b and 2c depict the converted echograms in dB using sonar equations from Mullison (2017) and RDI (1990). The scattering objects visualized in the echograms likely represent zooplankton and not total suspended solids (TSS) due to the study area's continuous water mass renewal, resulting in low TSS concentrations. Although both echograms exhibit similar patterns, detailed inspection reveals variations. The RDI (1990) sonar equation generates an echogram with a stronger acoustic backscatter signal response compared to Mullison's (2017) equation (Fig. 2b). This is evident from the brighter and thicker orange regions and the broader range of blue colors representing water depths in the RDI echogram. Consequently, Mullison's (2017) equation was chosen for further analysis based on this comparison.

Following Simmonds & MacLennan (2008), Bezerra-Neto et al. (2013), and Austin et al. (2022), a threshold range of -90 dB to -50 dB was applied to the echogram visualization derived from the sonar equation to identify zooplankton in the water column. The echogram in this study serves to visualize the presence and density of zooplankton based on the magnitude of the MVBS value. Strong acoustic backscatter signifies high zooplankton

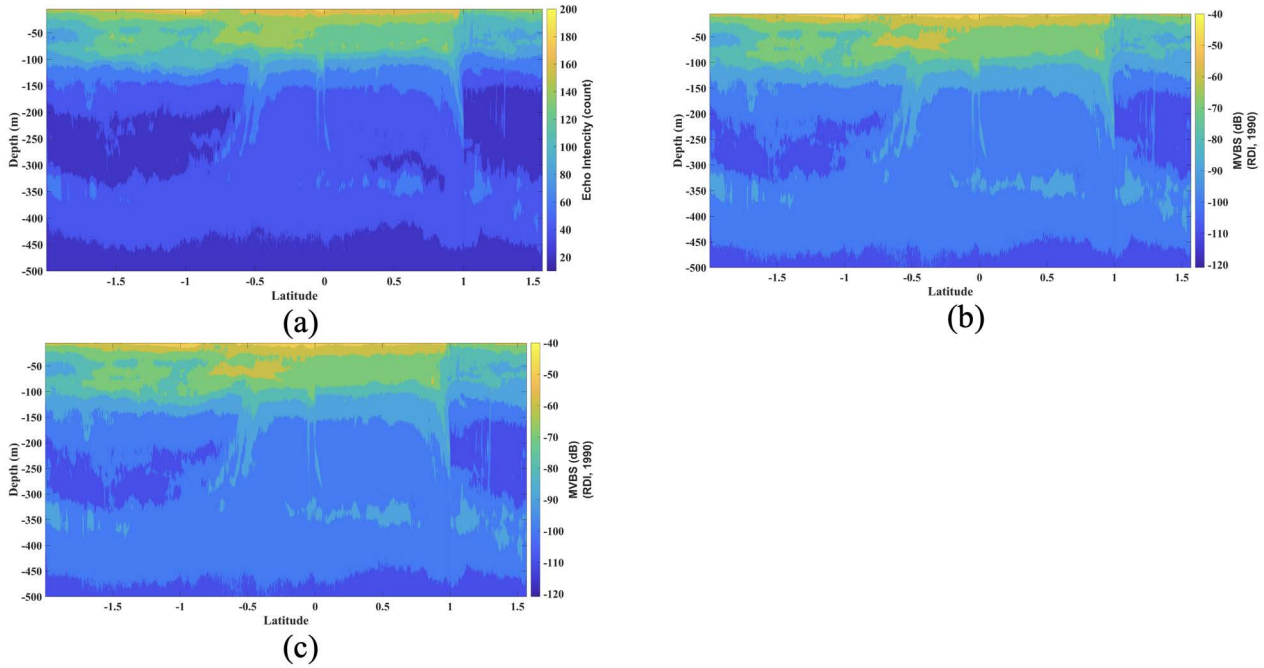

Figure 2. (a) Corrected EI value of SADCP through mean filter signal processing analysis. MVBS value by applying the formulation of (b) Mullison (2017) and (c) RDI (1990)

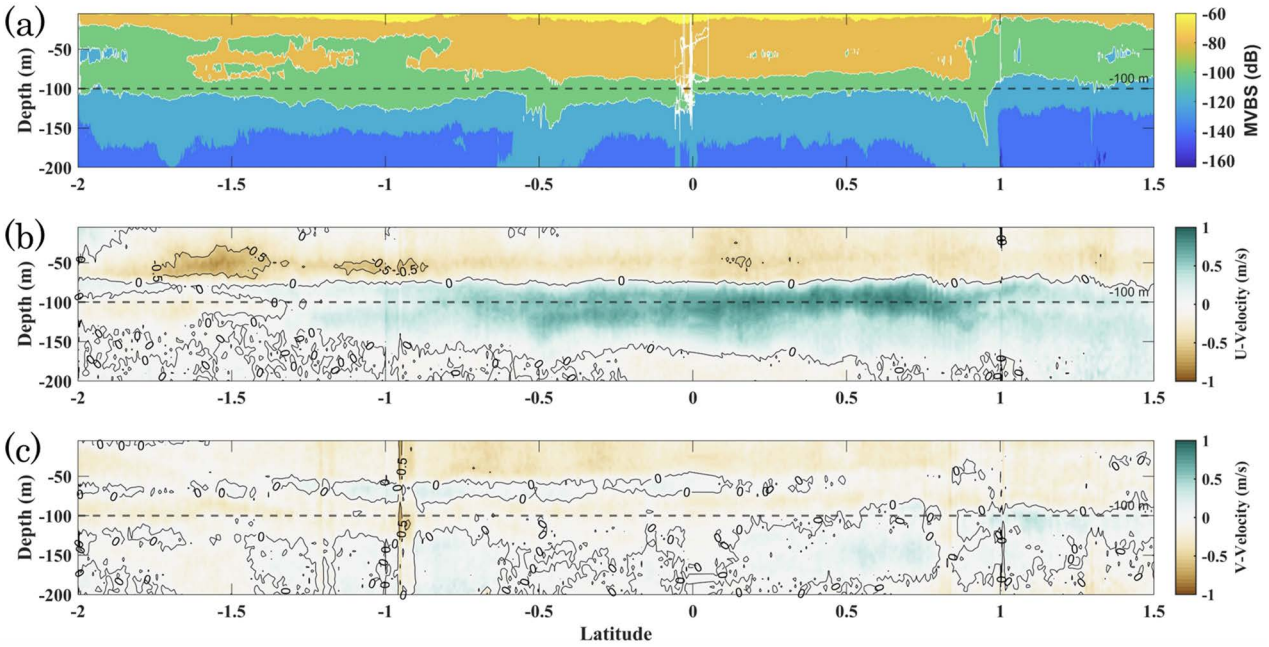

Figure 3. (a) Distribution of MVBS values and current velocity patterns (b) meridional and (c) transverse with depth

density, whereas weak backscatter indicates low density within the water column (Dwinovantyo et al., 2018; Zhang et al., 2004).

MVBS and Zooplankton Biomass Distribution in the Western Waters of Sumatra

Zooplankton, microscopic animals with limited swimming abilities, rely heavily on ocean currents for their distribution (Hays, 2017; Lawson et al., 2004). This study utilizes Spatial Acoustic Doppler Current Profiler (SADCP) data to examine zooplankton distribution patterns. The distribution of MVBS values from SADCP indicates a concentration of zooplankton along the survey track (Figure 3a). High MVBS values correspond to dense zooplankton aggregations, as confirmed by the echogram (Figure 3a). These dense patches are evident from the surface down to 100 m, with the

highest concentrations observed near the equator (latitudes -1° to 1°). Notably, the echogram reveals deeper zooplankton detection (down to 120 m) at these equatorial latitudes. The orange color on the echogram corresponds to high MVBS values, signifying high zooplankton patch density, while lighter blue areas indicate lower densities (Kim et al., 2016). Light penetration into the water column likely plays a role in these elevated MVBS values, potentially reflecting higher zooplankton abundance near the surface (Dwinovantyo et al., 2018; Manik, 2015).

Furthermore, the combined analysis of SSL thickness and MVBS values in Figure 3a indicates a zone of higher zooplankton density in the upper water column, primarily located above the Equatorial Undercurrent (EUC) at depths of approximately 80–120 m within the latitudinal range of -1° to 1°. This observation is consistent with the vertical overlap between the region of higher scattering layer (SSL) density and the core of the EUC, as illustrated in Figures 3b and 3c. The elevated zooplankton density above the EUC is likely influenced by the nutrient enrichment and physical stability provided by the undercurrent, which may create a favorable habitat for zooplankton aggregation. This stratified distribution highlights the dynamic interaction between physical oceanographic processes and biological patterns in the equatorial waters off the coast of Sumatra.

Spatial Acoustic Doppler Current Profiler (SADCP) data provides valuable insights into zooplankton distribution patterns (Figure 3a). However, it is important to acknowledge that MVBS calculations cannot differentiate between individual zooplankton species due to variations in their acoustic properties (Potiris et al., 2018). While MVBS offers a reliable estimate of total zooplankton biomass, it cannot distinguish specific species within a population. Nevertheless, studies by Wang et al. (2014) demonstrate that analyzing MVBS characterization and spatial distribution effectively reveals zooplankton abundance within the sound scattering layer (SSL). MVBS values are influenced not only by individual zooplankton size but also by their overall abundance within a specific water volume. The current processing techniques for zooplankton using MVBS offer sufficient sensitivity to detect their presence, with a threshold ranging from -140 to -60 dB (Figure 4a).

Figure 4b illustrates the vertical profile of current speed and direction in West Sumatran waters, spanning depths from the surface (5 m) to 300 m. The surface layer (0–70 m), particularly between latitudes 1°N and 2°N, exhibits a dominant westward-northwestward current with a maximum speed of 0.7 m/s. Interestingly, a localized current reversal occurs at latitude 2°N, with an eastward flow extending from the surface down to 50 m depth. The prevailing westward-northwestward current is primarily driven by the monsoonal winds, which typically switch direction around March each year (Singh & Roxy, 2022). These monsoon winds act as the key driver of surface circulation patterns in the equatorial waters west of Sumatra. Their influence is so strong that they cause a twice-yearly

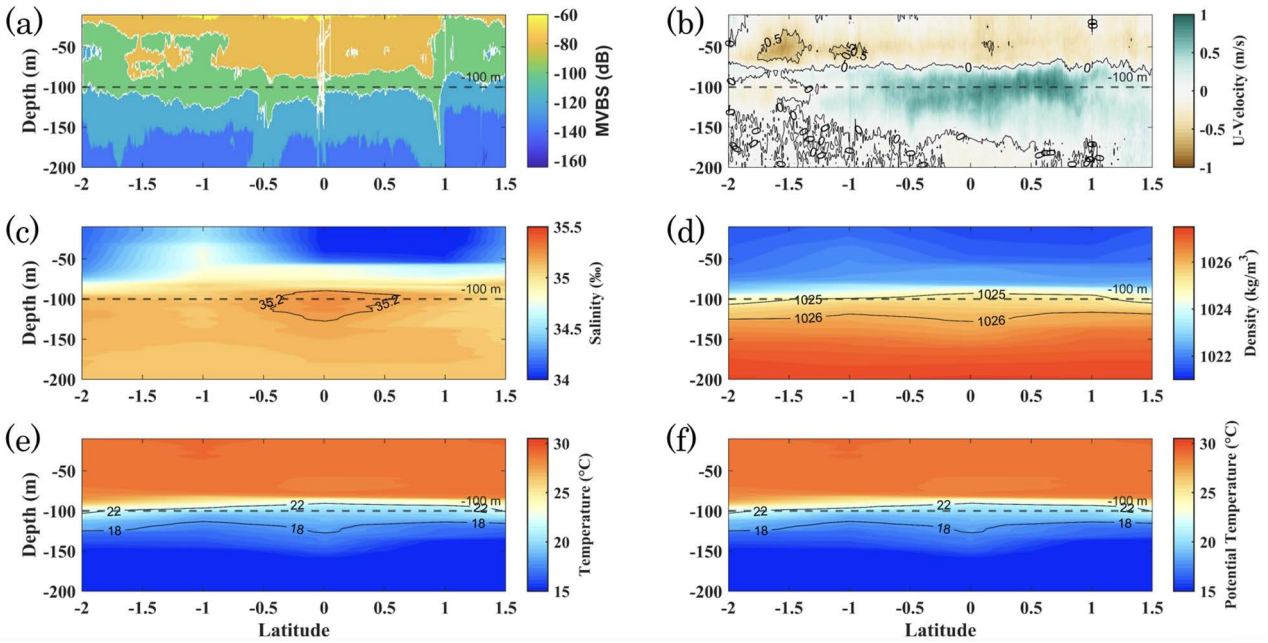

Figure 4. Distribution of (a) MVBS, (b) u-velocity, (c) salinity, (d) density, (e) temperature, and (f) potential temperature values with depth at 2°S to 2°N

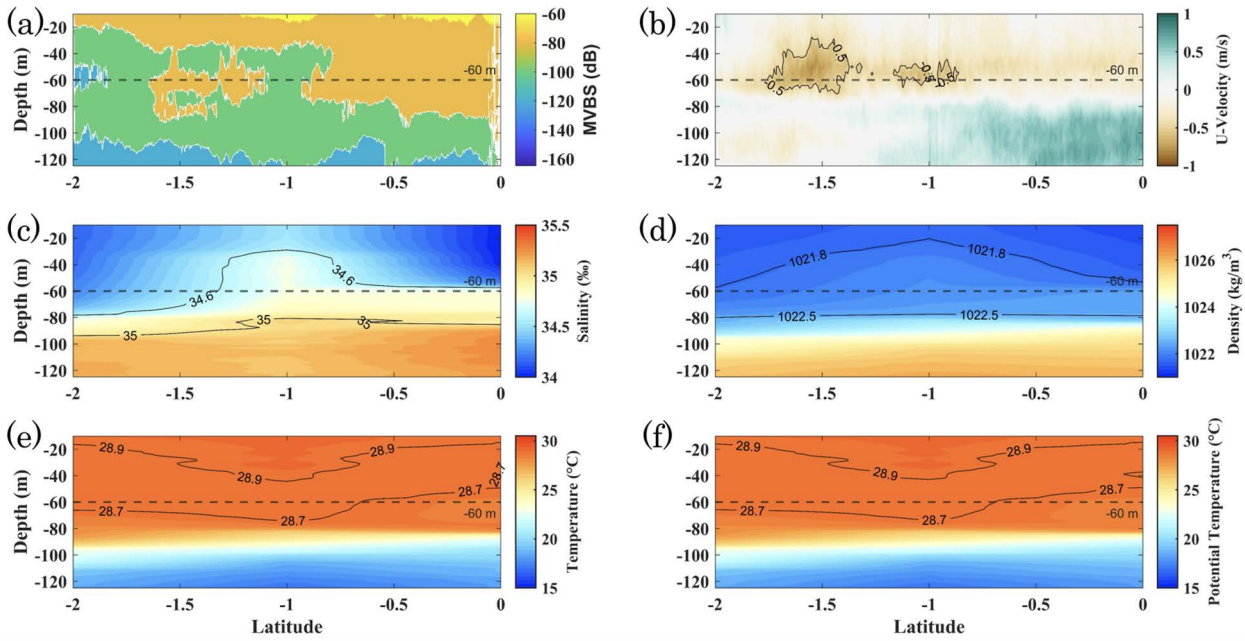

Figure 5. Distribution of (a) MVBS, (b) u-velocity, (c) salinity, (d) density, (e) temperature, and (f) potential temperature values with depth at 2°N to 0°

reversal of surface water mass circulation (Singh & Roxy, 2022).

At deeper layers (80 m to 150 m) between latitudes 1.2°N and 1.5°N (Figure 4b), a strong eastward current with a maximum velocity of 0.9 m/s becomes evident. This current corresponds to the Equatorial Undercurrent (EUC), which exhibits a stronger asymmetry towards the north of the equator, consistent with findings by Knauss & Taft (1964) and Kusmanto & Siswanto (2019). The EUC transports water masses with high salinity, reflecting its source in the western Sumatra region characterized by high salinity (35.0–35.2 PSU), low temperature (20–23°C), and high density (23–25 kg/m3) (Figures 4c–4f). Below 150 m depth, the current pattern transitions, with eastward dominance north of the equator and westward dominance with lower velocities south of the equator (Figure 4b).

The equatorial region hosts a strong eastward current, the Equatorial Undercurrent (EUC), at depths between 75 and 200 m (Figures 5a and 5b). This current arises from the pressure gradient generated by westward-moving surface Ekman currents, which are impeded by the Indian continent to the west. The resulting eastward flow is confined to a narrow band around the equator (roughly 1°N to 1°S) due to the Coriolis force. Notably, the EUC in West Sumatra exhibits an asymmetric trend, with a stronger flow south of the equator, potentially reflecting seasonal variations in monsoon winds (Xie et al., 2023).

The EUC plays a crucial role in shaping the water mass properties of the region. Eastward water movement at depths of 75 to 150 m around latitudes 1.2°S to 1.5°N suggests a change in flow direction compared to the overlying currents (Figure 5c). This eastward transport likely originates from the West Indian Ocean, contributing to higher salinity in the eastern equatorial waters (Figure 5c). The presence of a strong thermocline layer between 75 and 200 m (Figures 5d–5f) further reinforces stratification and limits vertical mixing.

The EUC's influence extends beyond water properties, potentially impacting zooplankton distribution. Zooplankton are primarily drifters, and the weak MVBS values observed during periods of high horizontal current velocities (Figures 5a and 5b) suggest a possible correlation. Additionally, the rise-and-fall patterns of MVBS and vertical velocity within the sound scattering layer (SSL) support zooplankton as the primary source of strong turbulence. However, MVBS and vertical velocity data cannot identify specific zooplankton species responsible for these signals.

Interestingly, low MVBS values at depths of 60 m between latitudes 1.5°S and 0.5°S coincide with westward currents flowing in a west-northwest direction at shallower depths (0–70 m) (Figures 5a and 5b). These westward currents, driven by the monsoonal winds, likely originate from the Indian Ocean and contribute to the observed low zooplankton distribution (Sprintall et al., 2000).

In contrast, the EUC in the Indian Ocean acts as a conduit for warmer (19°–21°C) and high-salinity (34.6–35.2 PSU) water masses from the eastern Indian Ocean, eventually flowing southward as the South Java Current (SJC) (Figures 5e–5f). The SJC traverses along the west coast of Sumatra, potentially influencing the surface water properties and contributing to the formation of a warm, low-zooplankton pool in southwest Sumatran waters.

CONCLUSSIONS

This study successfully employed Acoustic Doppler Current Profiler (ADCP) data to investigate zooplankton distribution and density in western Sumatra. Raw ADCP backscatter values, ranging from 20 to 160 counts, were converted into Mean Volume Backscattering Strength (MVBS) using sonar equations, facilitating analysis (MVBS: -160 dB to -60 dB). Spatial patterns revealed higher zooplankton densities at 100-200 m compared to shallower depths (0-100 m) and deeper depths (200-500 m). The equatorial undercurrent (EUC) influenced zooplankton distribution, transporting higher zooplankton biomass, warm temperatures (19°-21°C), and high salinity (34.6-35.2 PSU) from the surface layer (0-75 m) towards western Sumatra from the eastern Indian Ocean (depths: 75-170 m, speeds: 0.25-0.85 m/s). Temperature and salinity analyses indicated the influence of South Indian Central Water (SICW), characterized by high salinity levels (34.6–35.2 PSU). This high-salinity water mass was observed to positively correlate with zooplankton distribution. This suggests that areas with higher salinity are associated with greater zooplankton abundance. Notably, the observed EUC movement displayed an asymmetric northward strengthening trend. This study demonstrates the effectiveness of ADCP instruments in observing zooplankton distribution and behavior based on backscatter data, highlighting their utility in understanding current-mediated zooplankton transport and biomass variations.

ACKNOWLEDGEMENTS

The authors express gratitude to the Maritime Meteorology Center (BMKG) and the survey team of Research Vessel Baruna Jaya VIII for providing field measurement data, enabling the completion of this research.

REFERENCES

Ainslie, M. A., and McColm, J. G., 1998. A simplified formula for viscous and chemical absorption in sea water. *The Journal of the Acoustical Society of America*, *103*(3), 1671–1672. https://doi.org/10.1121/1.421258

Austin, J. A., Hrabik, T. R., and Branstrator, D., 2022. An abrupt decline in springtime zooplankton diel vertical migration due to a shift in stratification regime. *Journal of Great Lakes Research*, *48*(3), 837-842.

Bakhtiyar, Y., Arafat, M. Y., Andrabi, S., and Tak, H. I., 2020. Zooplankton: The Significant Ecosystem Service Provider in Aquatic Environment. *Bioremediation and Biotechnology, Vol 3: Persistent and Recalcitrant Toxic Substances*, *3*, 227–244. https://doi.org/10.1007/978-3-030-46075-4_10/COVER

Bezerra-Neto, J. F., Brighenti, L. S., and Pinto-Coelho, R. M., 2013. Implementation of hydroacoustic for a rapid assessment of fish spatial distribution at a Brazilian Lake-Lagoa Santa, MG. *Acta Limnologica Brasiliensia*, *25*, 91-98.

Cheng, X. W., Zhang, L. L., Gao, F., Tan, Y. H., Xiang, R., Qiu, Z. Y., and He, L. J., 2022. Biodiversity of zooplankton in 0–3000 m waters from the eastern Indian Ocean in spring 2019 based on metabarcoding. *Water Biology and Security*, *1*(1), 100005. https://doi.org/10.1016/J.WATBS.2022.100005

Chun, S., La, H. S., Son, W., Kim, Y. C., Cho, K. H., and Yang, E. J., 2022. Detection method for diel vertical migration pattern using 2D cross-correlation with ADCP backscatter time-series data. *Methods in Ecology and Evolution*, *13*(7), 1475–1487. https://doi.org/10.1111/2041-210X.13871

Cisewski, B., Strass, V. H., Rhein, M., and Krägefsky, S., 2010. Seasonal variation of diel vertical migration of zooplankton from ADCP backscatter time series data in the Lazarev Sea, Antarctica. *Deep Sea Research Part I: Oceanographic Research Papers*, *57*(1), 78–94. https://doi.org/10.1016/J.DSR.2009.10.005

Cisewski, B., and Strass, V. H., 2016. Acoustic insights into the zooplankton dynamics of the eastern Weddell Sea. *Progress in*

Oceanography, *144*, 62–92. https://doi.org/10.1016/J.POCEAN.2016.03.005

Deines, K. L., 1999. Backscatter estimation using broadband acoustic Doppler current profilers. *Proceedings of the IEEE Working Conference on Current Measurement*, 249–253. https://doi.org/10.1109/CCM.1999.755249

Dwinovantyo, A., Manik, H. M., Prartono, T., and Susilohadi., 2018. Application of Acoustic Doppler Current Profiler (ADCP) to Observe Diel Vertical Migration of Zooplankton. *Journal of Physics: Conference Series*, *1075*(1), 012016. https://doi.org/10.1088/1742-6596/1075/1/012016

Espinasse, B., Pagano, M., Basedow, S. L., Chevalier, C., Malengros, D., and Carlotti, F., 2023. Water column distribution of zooplanktonic size classes derived from in-situ plankton profilers: Potential use to contextualize contaminant loads in plankton. *Marine Pollution Bulletin*, *196*, 115573. https://doi.org/10.1016/J.MARPOLBUL.2023.115573

Flagg, C. N., and Smith, S. L., 1989. On the use of the acoustic Doppler current profiler to measure zooplankton abundance. *Deep Sea Research Part A. Oceanographic Research Papers*, *36*(3), 455-474.

Gartner, J. W., 2004. Estimating suspended solids concentrations from backscatter intensity measured by acoustic Doppler current profiler in San Francisco Bay, California. *Marine Geology*, *211*(3-4), 169-187.

Guerra, D., Schroeder, K., Borghini, M., Camatti, E., Pansera, M., Schroeder, A., Sparnocchia, S., and Chiggiato, J., 2019. Zooplankton diel vertical migration in the Corsica Channel (north-western Mediterranean Sea) detected by a moored acoustic Doppler current profiler. *Ocean Science*, *15*(3), 631–649. https://doi.org/10.5194/OS-15-631-2019

Hays, G. C., 2017. Ocean currents and marine life. *Current Biology*, *27*(11), R470–R473. https://doi.org/10.1016/j.cub.2017.01.044

Heywood, K. J., Scrope-Howe, S., and Barton, E. D., 1991. Estimation of zooplankton abundance from shipborne ADCP backscatter. *Deep Sea Research Part A. Oceanographic Research Papers*, *38*(6), 677–691. https://doi.org/10.1016/0198-0149(91)90006-2

Holliday, D. V., Pieper, R. E., and Kleppel, G. S., 1989. Determination of zooplankton size and distribution with multifrequency acoustic technology. *ICES Journal of Marine Science*, *46*(1), 52–61. https://doi.org/10.1093/ICESJMS/46.1.52

Kang, M., Furusawa, M., and Miyashita, K., 2002. Effective and accurate use of difference in mean volume backscattering strength to identify fish and plankton. *ICES Journal of Marine Science*, *59*(4), 794–804. https://doi.org/10.1006/JMSC.2002.1229

Kim, E., Mukai, T., and Iida, K., 2016. Acoustic identification of krill and copepods using frequency differences of volume backscattering strength around Funka Bay, Hokkaido, Japan. *Nippon Suisan Gakkaishi (Japanese Edition)*, *82*(4), 587–600. https://doi.org/10.2331/SUISAN.15-00039

Knauss, J. A., and Taft, B. A., 1964. Equatorial Undercurrent of the Indian Ocean. *Science (New York, N.Y.)*, *143*(3604), 354–356. https://doi.org/10.1126/SCIENCE.143.3604.354

Kusmanto, E., and Siswanto, S., 2019. Analisis Masa Air Dan Estimasi Transport Arus Bawah Ekuator Pada Bujur 90°E Selama Indonesia Prima 2017. *Jurnal Meteorologi Dan Geofisika*, *19*(2), 59. https://doi.org/10.31172/JMG.V19I2.522

La, H. S., Ha, H. K., Kang, C. Y., Wåhlin, A. K., and Shin, H. C., 2015. Acoustic backscatter observations with implications for seasonal and vertical migrations of zooplankton and nekton in the Amundsen shelf (Antarctica). *Estuarine, Coastal and Shelf Science*, *152*, 124–133. https://doi.org/10.1016/J.ECSS.2014.11.020

Lawson, G. L., Wiebe, P. H., Ashjian, C. J., Gallager, S. M., Davis, C. S., and Warren, J. D., 2004. Acoustically-inferred zooplankton distribution in relation to hydrography west of the Antarctic Peninsula. *Deep Sea Research Part II: Topical Studies in Oceanography*, *51*(17–19), 2041–2072. https://doi.org/10.1016/J.DSR2.2004.07.022

Lee, K., Mukai, T., Lee, D., and Iida, K., 2008. Verification of mean volume backscattering strength obtained from acoustic Doppler

current profiler by using sound scattering layer. *Fisheries Science*, *74*(2), 221–229. https://doi.org/10.1111/J.1444-2906.2008.01516.X/METRICS

Lee, K., Mukai, T., Lee, D. J., and Iida, K., 2014. Classification of sound-scattering layers using swimming speed estimated by acoustic Doppler current profiler. *Fisheries Science*, *80*(1), 1–11. https://doi.org/10.1007/S12562-013-0683-9/FIGURES/7

Lomartire, S., Marques, J. C., and Gonçalves, A. M. M., 2021. The key role of zooplankton in ecosystem services: A perspective of interaction between zooplankton and fish recruitment. *Ecological Indicators*, *129*, 107867. https://doi.org/10.1016/J.ECOLIND.2021.107867

Lyons, A. B., and Parish, C. R., 1994. Determination of lymphocyte division by flow cytometry. *Journal of Immunological Methods*, *171*(1), 131–137. https://doi.org/10.1016/0022-1759(94)90236-4

Mackenzie, K. V., 1981. Nine-term equation for sound speed in the oceans. *The Journal of the Acoustical Society of America*, *70*(3), 807–812. https://doi.org/10.1121/1.386920

Manik, H. M., 2015. Acoustic Observation of Zooplankton Using High Frequency Sonar (Observasi Akustik Zooplankton Menggunakan Sonar Frekuensi Tinggi). *ILMU KELAUTAN: Indonesian Journal of Marine Sciences*, *20*(2), 61–72. https://doi.org/10.14710/IK.IJMS.20.2.61-72

Manik, H. M., and Firdaus, R., 2021. Quantifying suspended sediment using acoustic doppler current profiler in Tidung island seawaters. *Pertanika Journal of Science and Technology*, *29*(1), 363–385. https://doi.org/10.47836/PJST.29.1.21

Manso-Narvarte, I., Fredj, E., Jordà, G., Berta, M., Griffa, A., Caballero, A., and Rubio, A., 2020. 3D reconstruction of ocean velocity from high-frequency radar and acoustic Doppler current profiler: A model-based assessment study. *Ocean Science*, *16*(3), 575–591. https://doi.org/10.5194/OS-16-575-2020

Mohn, C., Denda, A., Christiansen, S., Kaufmann, M., Peine, F., Springer, B., Turnewitsch, R., and Christiansen, B., 2018. Ocean currents and acoustic backscatter data from shipboard ADCP measurements at three North Atlantic seamounts between 2004 and 2015. *Data in Brief*, *17*, 237–245. https://doi.org/10.1016/J.DIB.2018.01.014

Mullison, J. W., 2017. Backscatter estimation using broadband acoustic doppler current profilers-updated. *Proceedings of the ASCE Hydraulic Measurements & Experimental Methods Conference, Durham, NH, USA*, 9–12.

Mullison, J. W., 2019. Backscatter Estimation Using ADCPs - Twenty Years Later. *2019 IEEE/OES 12th Current, Waves and Turbulence Measurement, CWTM 2019*. https://doi.org/10.1109/CWTM43797.2019.8955274

Nava, V., and Leoni, B., 2021. A critical review of interactions between microplastics, microalgae and aquatic ecosystem function. *Water Research*, *188*, 116476. https://doi.org/10.1016/J.WATRES.2020.116476

Potiris, E., Frangoulis, C., Kalampokis, A., Ntoumas, M., Pettas, M., Petihakis, G., and Zervakis, V., 2018. Acoustic Doppler current profiler observations of migration patternsof zooplankton in the Cretan Sea. *Ocean Science*, *14*(4), 783–800. https://doi.org/10.5194/OS-14-783-2018

RDI., 1990. Calculating absolute backscatter. *RD Instruments Technical Bulletin ADCP-90-04, 24pp*.

Receveur, A., Kestenare, E., Allain, V., Ménard, F., Cravatte, S., Lebourges-Dhaussy, A., Lehodey, P., Mangeas, M., Smith, N., Radenac, M. H., and Menkes, C., 2020. Micronekton distribution in the southwest Pacific (New Caledonia) inferred from shipboard-ADCP backscatter data. *Deep Sea Research Part I: Oceanographic Research Papers*, *159*, 103237. https://doi.org/10.1016/J.DSR.2020.103237

Schiano, E., Pensieri, S., Bozzano, R., and Picco, P., 2013. Analysis of long time series of ADCP backscatter data in the Ligurian Sea to investigate the zooplankton variability. *OCEANS 2013 MTS/IEEE Bergen: The Challenges of the Northern Dimension*. https://doi.org/10.1109/OCEANS-BERGEN.2013.6608040

Simmonds, J., and MacLennan, D., 2008. Fisheries acoustics: Theory and practice: Second edition. *Fisheries Acoustics: Theory and*

Practice: Second Edition, 1–252. https://doi.org/10.1002/9780470995303

Singh, V. K., and Roxy, M. K., 2022. A review of ocean-atmosphere interactions during tropical cyclones in the north Indian Ocean. *Earth-Science Reviews*, *226*, 103967. https://doi.org/10.1016/J.EARSCIREV.2022.103967

Song, Y., Yang, J., Wang, C., and Sun, D., 2022. Spatial patterns and environmental associations of deep scattering layers in the northwestern subtropical Pacific Ocean. *Acta Oceanologica Sinica*, *41*(7), 139–152. https://doi.org/10.1007/S13131-021-1973-1/METRICS

Sprintall, J., Gordon, A. L., Murtugudde, R., and Susanto, R. D., 2000. A semiannual Indian Ocean forced Kelvin wave observed in the Indonesian seas in May 1997. *Journal of Geophysical Research: Oceans*, *105*(C7), 17217–17230. https://doi.org/10.1029/2000JC900065

Szczucka, J., Trudnowska, E., Hoppe, L., and Błachowiak-Samołyk, K., 2016. Comparison of acoustical and optical zooplankton measurements using an acoustic scattering model: A case study from the Arctic frontal zone. *Polish Polar Research*, *37*(1), 67–88. https://doi.org/10.1515/POPORE-2016-0008

Thoman, T. X., Kukulka, T., Cohen, J. H., and Boettcher, H., 2023. Zooplankton-microplastic exposure in Delaware coastal waters: Atlantic blue crab (Callinectes sapidus) larvae case study. *Marine Pollution Bulletin*, *196*, 115541. https://doi.org/10.1016/J.MARPOLBUL.2023.115541

Urick, R. J., 1984. *Ambient noise in the sea*. Undersea Warfare Technology Office, Naval Sea Systems Command, Department of the Navy.

Vogel, M., Silveira, I. C. A., Castro, B. M., Lima, J. A. M., Pereira, A. F., and Williams, P., 2010. Metocean Measurements at Northern Santos Basin - Brazil. *Proceedings of the Annual Offshore Technology Conference*, *4*, 2967–2978. https://doi.org/10.4043/20947-MS

Wang, Z., DiMarco, S. F., Ingle, S., Belabbassi, L., and Al-Kharusi, L. H., 2014. Seasonal and annual variability of vertically migrating scattering layers in the northern Arabian Sea. *Deep Sea Research Part I: Oceanographic Research Papers*, *90*(1), 152–165. https://doi.org/10.1016/J.DSR.2014.05.008

Woodgate, R. A., and Holroyd, A. E., 2011. Correction of Teledyne Acoustic Doppler Current Profiler (ADCP) bottom-track range measurements for instrument pitch and roll. *arXiv preprint arXiv:1110.5003*.

Wormuth, J. H., Ressler, P. H., Cady, R. B., Harris, E. J., Ressler, P. H., Cady, R. B., and Harris, E. J., 2000. Zooplankton and Micronekton in Cyclones and Anticyclones in the Northeast Gulf of Mexico. *Gulf of Mexico Science*, *18*(1), 3. https://doi.org/10.18785/goms.1801.03

Xie, C., Ding, R., Xuan, J., and Huang, D., 2023. Interannual variations in salt flux at 80°E section of the equatorial Indian Ocean. *Science China Earth Sciences*, *66*(9), 2142–2161. https://doi.org/10.1007/S11430-022-1140-X/METRICS

Zhang, L., Zhou, W., and Jiao, L., 2004. Wavelet Support Vector Machine. *IEEE Transactions on Systems, Man, and Cybernetics, Part B: Cybernetics*, *34*(1), 34–39. https://doi.org/10.1109/TSMCB.2003.811113